—Supporting Information—
Accuracy of metaGGA functionals in describing transition metal fluorides

Dereje Bekele Tekliye[1] and Gopalakrishnan Sai Gautam[1,*]

[1]Department of Materials Engineering, Indian Institute of Science, Bengaluru, 560012, India
[*]Email: saigautamg@iisc.ac.in

Oxidation energetics of Cr and Mn fluorides

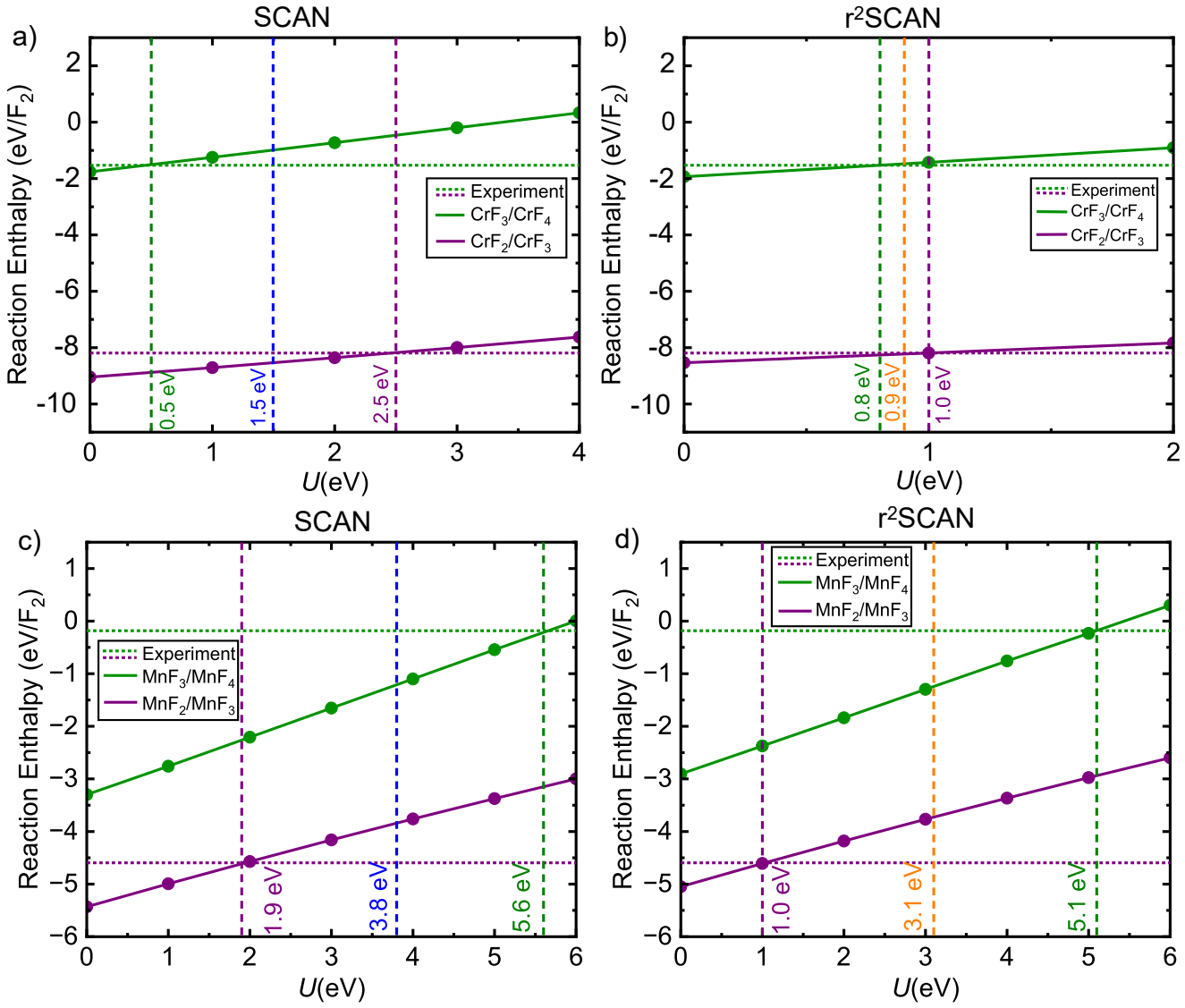

Figure S1: Variation of fluorination reaction enthalpy (solid line) with increasing U in the Hubbard U corrected strongly constrained and appropriately normed (SCAN+U, panels a and c) and the U corrected restored regularized SCAN (r^{2}SCAN+U, panels b and d) frameworks Cr (panels a and b) and Mn (panels c and d). Horizontal dotted line of a given colour in each panel reflects the experimental oxidation enthalpy for the reaction considered, with the vertical dashed line of the same colour signifying the U value that minimizes error between SCAN+U/r^{2}SCAN+U predictions and experiments for the respective reaction. Vertical blue and orange dashed lines indicate optimal U (magnitude is annotated as text with the same colour as the line) for SCAN+U and r^{2}SCAN+U functionals, respectively.

Magnetic configuration of transition metal fluorides (TMFs)

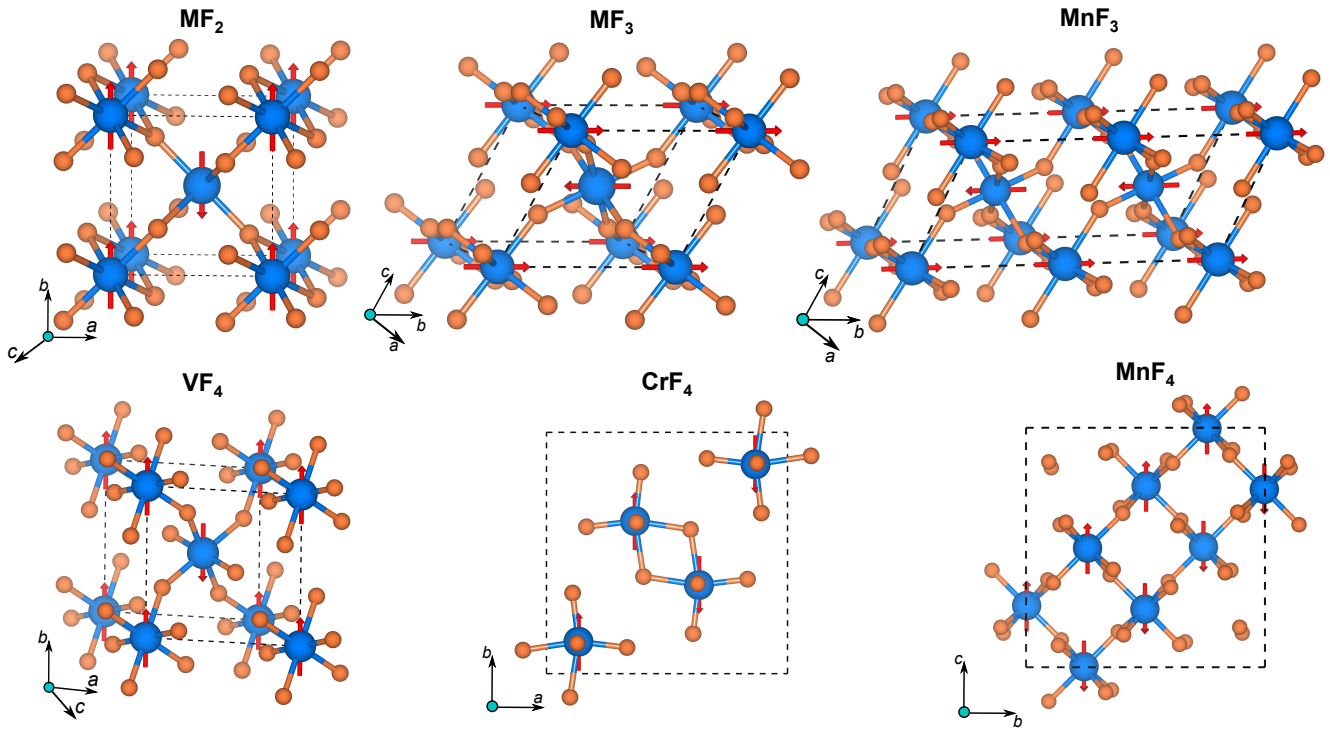

Figure S2: The ground state ordering of magnetic moments on the transition metal (TM) ions in TMFs. The light blue and orange spheres represent the TM and F atoms, respectively. M in MF_2 represents Cr, Mn, Fe, Co, Ni, or Cu, while M in MF_3 signifies Ti, V, Cr, Fe, Co, or Ni. Red arrows indicate the direction of magnetic moments on TMs. All the structures presented here have similar antiferromagnetic (AFM) (G-type or ↑↓↑↓) ordering, except MnF_3 which has an A-type AFM (↑↑↓↓) ordering. Note that NiF_3 exhibits a ferromagnetic (FM) ground state in preference to the AFM configuration displayed here. CuF and TiF_4 are non-magnetic and are not presented here.

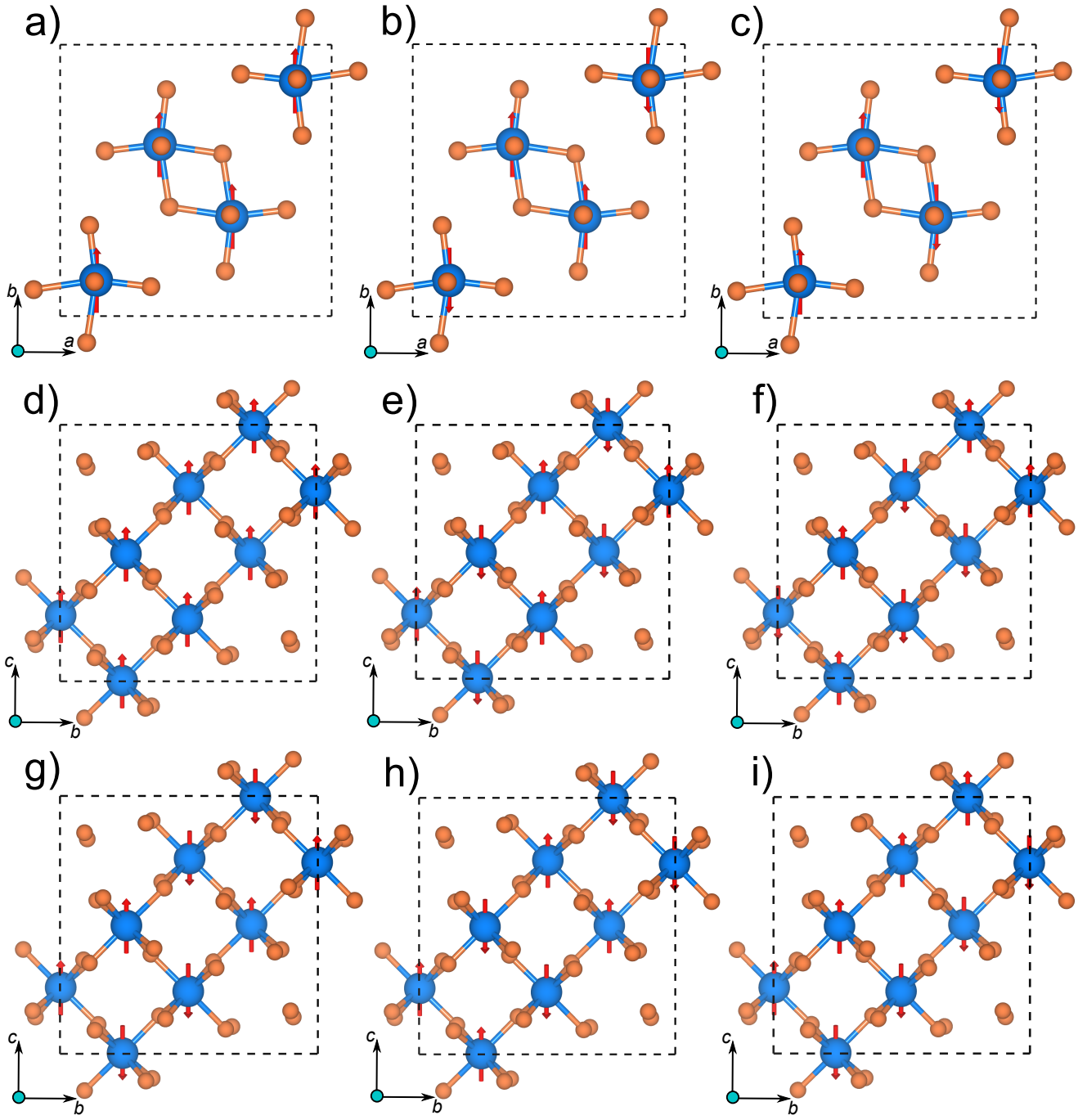

Figure S3: Different ferromagnetic and AFM orderings of CrF_4 (panels a-c) and MnF_4 (panels d-i) considered in our calculations. All notations used in this Figure are similar to Figure S2. Panel c and i are the SCAN-calculated ground states for CrF_4 and MnF_4, respectively.

Oxidation energetics of Ni and Cu fluorides

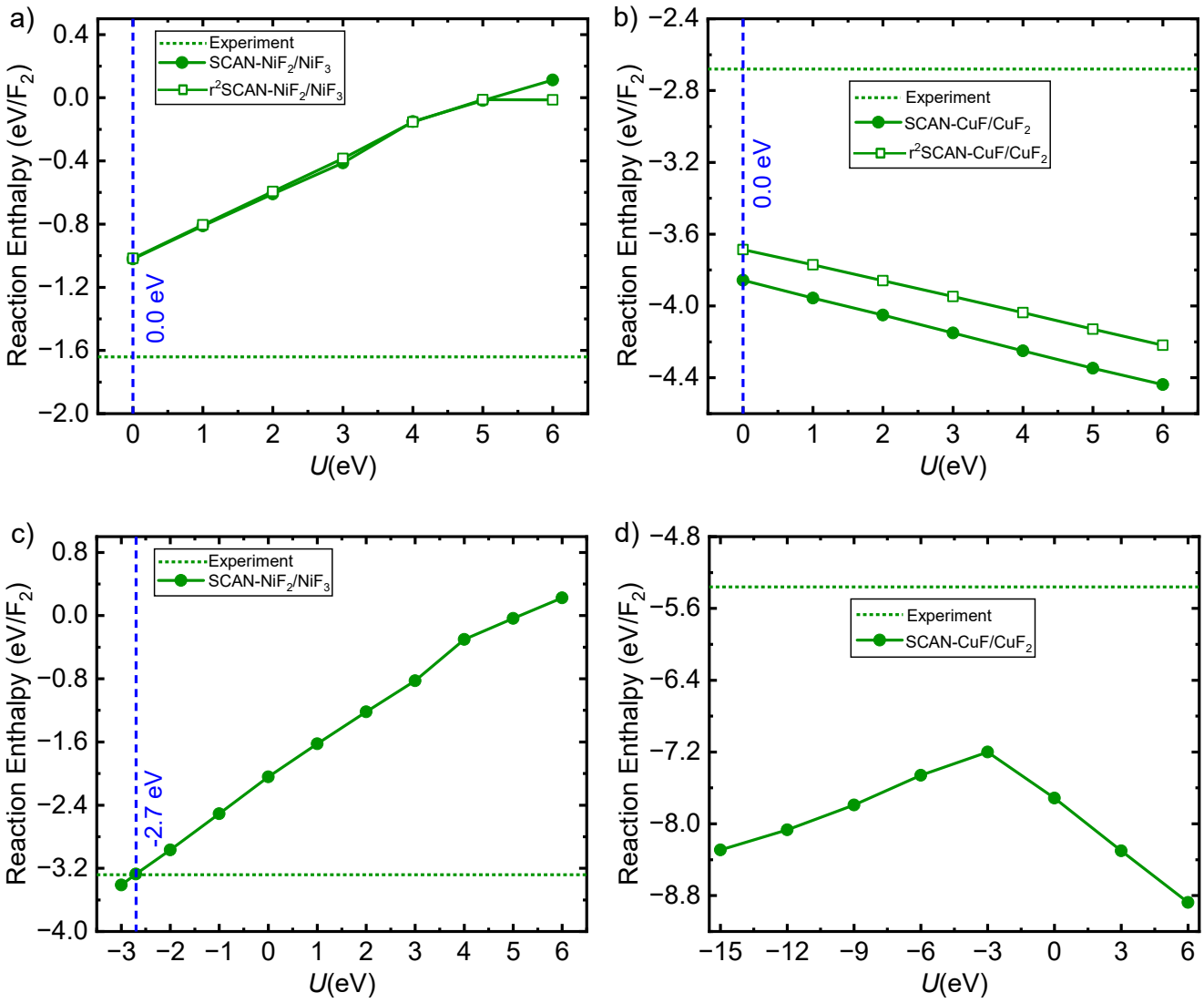

Figure S4: Oxidation enthalpy versus applied U within the SCAN+U and r^{2}SCAN+U frameworks for (a) Ni and (b) Cu fluorides. Oxidation enthalpy versus applied U for a wider range of -3 to 6 eV for (c) Ni and -15 to 6 eV for (d) Cu fluorides within the SCAN+U framework. Notations on the plot are similar to those used in Figure 2 of the main text.

Projector Augmented Wave potentials

Table S1: Projector augmented wave potentials used to describe the core electrons in our calculations.

Element	**Potential**
Ti	Ti_pv 07Sep2000
V	V_pv 07Sep2000
Cr	Cr_pv 02Aug2007
Mn	Mn_pv 02Aug2007
Fe	Fe_pv 02Aug2007
Co	Co_pv 23Apr2009
Ni	Ni_pv 06Sep2000
Cu	Cu_pv 06Sep2000
Na	Na_pv 19Sep2006
F	F 08Apr2002

Optimized U with data at 298 K and 0 K

Table S2: Experimental enthalpy of formation at 0 K extrapolated from enthalpy measured at high temperature ($\geq$ 298 K) as presented in [1] and the corresponding calculated U value of $3d$ transition metal fluorides (TMFs) for SCAN+U and r^{2}SCAN+U.

Compound	ΔH_f^{expt}	U (eV)	
	(eV/atom) at 0 K	SCAN+U	r^{2}SCAN+U
TiF_3	-3.713	4.5	4.5
TiF_4	-3.414		
VF_3	-3.272	3.0	3.3
VF_4	-2.904		
CrF_2	-2.687		
CrF_3	-2.997	1.7	1.1
CrF_4	-2.581		
MnF_2	-2.954		
MnF_3	-2.770	3.9	3.2
MnF_4	-2.239		
FeF_2	-2.479	3.6	3.5
FeF_3	-2.628		
CoF_2	-2.323	3.7	5.2
CoF_3	-2.043		

Lattice parameters, on-site magnetic moments, and band gaps

Table S3: Experimental, SCAN, SCAN+U, r^{2}SCAN, and r^{2}SCAN+U lattice constants (Å), lattice angles (°), band gaps (eV), and average on-site magnetic moments (μ_B, on the $3d$ ions) of all the TMFs considered in this work. The structural space group is also listed for all compositions.

Composition (space group)	Source	Lattice constants (Å)			Lattice angles (°)			Band gap (eV)	On-site magnetic moment (μ_B)
		a	b	c	α	β	γ		
TiF_3	Expt.	5.52	5.52	5.52	59.1	59.1	59.1	_	0.0
($R\bar{3}cR$)	SCAN	5.48	5.43	5.51	58.6	59.1	58.8	0.19	0.9
	SCAN+U	5.59	5.51	5.63	58.6	59.0	58.6	3.71	0.9
	r^{2}SCAN	5.48	5.46	5.53	58.7	59.0	58.8	0.19	0.9
	r^{2}SCAN+U	5.60	5.53	5.64	58.5	59.0	58.6	3.68	0.9
TiF_4	Expt.	22.81	3.85	9.57	90.0	90.0	90.0	_	_
($Pnma$)	SCAN	22.26	3.86	9.47	90.0	90.0	90.0	4.37	0.0
	SCAN+U	22.38	3.91	9.51	90.0	90.0	90.0	4.72	0.0
	r^{2}SCAN	22.43	3.87	9.51	90.0	90.0	90.0	4.37	0.0
	r^{2}SCAN+U	22.52	3.93	9.56	90.0	90.0	90.0	4.73	0.0
VF_3	Expt.	5.37	5.37	5.37	57.5	57.5	57.5	_	2.0 [2]
($R\bar{3}cR$)	SCAN	5.34	5.34	5.33	57.1	57.1	57.2	0.75	1.8
	SCAN+U	5.41	5.41	5.41	57.5	57.6	57.6	3.84	1.9
	r^{2}SCAN	5.37	5.37	5.37	57.5	57.5	57.5	0.58	1.8
	r^{2}SCAN+U	5.44	5.44	5.44	57.5	57.5	57.5	3.88	1.9
VF_4	Expt.	5.38	5.17	5.34	90.0	59.7	90.0	_	1.0 [3]
($P21/c$	SCAN	5.29	5.16	5.27	90.0	60.5	90.0	1.18	1.0
	SCAN+U	5.34	5.20	5.30	90.0	60.7	90.0	3.54	1.0
	r^{2}SCAN	5.32	5.16	5.30	90.0	60.3	90.0	1.14	1.0
	r^{2}SCAN+U	5.36	5.21	5.32	90.0	60.6	90.0	3.64	1.0
CrF_2	Expt.	4.73	4.72	3.50	90.0	96.5	90.0	_	3.6 [4]
($P21/c$	SCAN	4.68	4.62	3.58	90.0	97.6	90.0	1.68	3.7
	SCAN+U	4.70	4.68	3.52	90.0	95.7	90.0	2.24	3.7
	r^{2}SCAN	4.71	4.67	3.57	90.0	97.7	90.0	1.47	3.7
	r^{2}SCAN+U	4.71	4.68	3.56	90.0	96.8	90.0	2.20	3.7
CrF_3	Expt.	5.26	5.26	5.26	56.6	56.6	56.6	_	3.0 [2]
($R\bar{3}cR$)	SCAN	5.24	5.24	5.24	57.0	57.0	57.0	1.90	2.8

Continued on next page

Table S3: Experimental, SCAN, SCAN+U, r^{2}SCAN, and r^{2}SCAN+U lattice constants (Å), lattice angles (°), band gaps (eV), and average on-site magnetic moments (μ_B, on the $3d$ ions) of all the TMFs considered in this work. The structural space group is also listed for all compositions. (Continued)

	SCAN+U	5.26	5.26	5.26	57.0	57.0	57.0	2.24	2.8
	r^{2}SCAN	5.25	5.25	5.25	56.9	56.9	56.9	1.59	2.8
	r^{2}SCAN+U	5.27	5.27	5.27	56.9	56.9	56.9	2.24	2.8
CrF_4	Expt.	8.30	8.30	3.74	90.0	90.0	90.0	_	_
(*P42/mnm*)	SCAN	8.07	8.07	3.78	90.0	90.0	90.0	0.00	1.9
	SCAN+U	8.10	8.10	3.79	90.0	90.0	90.0	0.30	2.0
	r^{2}SCAN	8.14	8.14	3.79	90.0	90.0	90.0	0.21	2.0
	r^{2}SCAN+U	8.13	8.11	3.80	90.0	90.0	90.0	0.41	2.0
MnF_2	Expt.	4.87	4.87	3.31	90.0	90.0	90.0	_	5.0 [5]
(*P42/mnm*)	SCAN	4.85	4.85	3.30	90.0	90.0	90.0	2.60	4.9
	SCAN+U	4.87	4.87	3.31	90.0	90.0	90.0	3.89	4.7
	r^{2}SCAN	4.86	4.86	3.30	90.0	90.0	90.0	2.74	4.6
	r^{2}SCAN+U	4.89	4.89	3.32	90.0	90.0	90.0	3.81	4.7
MnF_3	Expt.	10.07	5.12	5.29	63.7	61.6	60.5	_	4.0 [2]
(*C12/c1*)	SCAN	9.80	5.02	5.27	64.7	62.3	60.8	1.06	3.6
	SCAN+U	9.80	5.04	5.29	64.4	62.4	61.0	2.56	3.8
	r^{2}SCAN	9.88	5.06	5.28	64.3	62.1	60.8	0.89	3.7
	r^{2}SCAN+U	9.92	5.09	5.29	64.0	62.0	60.9	2.08	3.8
MnF_4	Expt.	12.63	12.63	6.05	90.0	90.0	90.0	_	3.9 [6]
(*I41/a*)	SCAN	5.93	9.36	9.36	84.3	71.6	71.5	2.18	2.6
	SCAN+U	5.95	9.40	9.41	84.3	71.6	71.6	2.41	2.9
	r^{2}SCAN	5.98	9.39	9.39	84.2	71.4	71.4	1.86	2.7
	r^{2}SCAN+U	5.98	9.44	9.44	84.2	71.5	71.5	2.13	2.9
FeF_2	Expt.	4.70	4.70	3.31	90.0	90.0	90.0	_	3.8 [7]
(*P42/mnm*)	SCAN	4.65	4.65	3.30	90.0	90.0	90.0	0.88	3.7
	SCAN+U	4.70	4.70	3.30	90.0	90.0	90.0	3.57	3.8
	r^{2}SCAN	4.66	4.66	3.32	90.0	90.0	90.0	0.94	3.7
	r^{2}SCAN+U	4.72	4.72	3.30	90.0	90.0	90.0	3.54	3.8
FeF_3	Expt.	5.36	5.36	5.36	57.9	57.9	57.9	_	5.0 [2]
($R\bar{3}cR$)	SCAN	5.36	5.36	5.36	57.9	57.9	57.9	2.62	4.2
	SCAN+U	5.36	5.36	5.36	57.9	57.9	57.9	5.27	4.5
	r^{2}SCAN	5.37	5.37	5.37	57.9	57.9	57.9	2.67	4.2

Continued on next page

Table S3: Experimental, SCAN, SCAN+U, r^{2}SCAN, and r^{2}SCAN+U lattice constants (Å), lattice angles (°), band gaps (eV), and average on-site magnetic moments (μ_B, on the $3d$ ions) of all the TMFs considered in this work. The structural space group is also listed for all compositions. (Continued)

	r^{2}SCAN+U	5.37	5.37	5.37	57.9	57.9	57.9	5.20	4.5
CoF_2	Expt.	4.70	4.70	3.18	90.0	90.0	90.0	_	2.6 [8]
(*P42/mnm*)	SCAN	4.65	4.65	3.18	90.0	90.0	90.0	1.59	2.7
	SCAN+U	4.68	4.68	3.18	90.0	90.0	90.0	4.58	2.8
	r^{2}SCAN	4.66	4.66	3.19	90.0	90.0	90.0	1.44	2.7
	r^{2}SCAN+U	4.69	4.69	3.18	90.0	90.0	90.0	4.92	2.9
CoF_3	Expt.	5.28	5.28	5.28	57.0	57.0	57.0	_	3.2 [9]
($R\bar{3}cR$)	SCAN	5.22	5.30	5.31	56.3	55.4	55.4	0.75	3.1
	SCAN+U	5.26	5.25	5.28	55.7	55.8	55.2	2.93	3.4
	r^{2}SCAN	5.31	5.26	5.33	55.9	56.5	56.0	0.71	3.1
	r^{2}SCAN+U	5.22	5.31	5.28	56.4	56.0	56.0	3.23	3.4
NiF_2	Expt.	4.65	4.65	3.08	90.0	90.0	90.0	_	2.0 [10]
(*P42/mnm*)	SCAN	4.62	4.62	3.05	90.0	90.0	90.0	2.83	1.7
	r^{2}SCAN	4.63	4.63	3.06	90.0	90.0	90.0	2.78	1.7
NiF_3	Expt.	5.53	7.70	5.37	90.0	90.0	90.0	_	_
($R\bar{3}R$)	SCAN	5.11	5.11	5.11	55.5	55.5	55.5	0.41	1.6
	r^{2}SCAN	5.11	5.11	5.11	55.5	55.5	55.5	0.43	1.6
CuF	Expt.	6.69	6.69	6.69	60.0	60.0	60.0	_	0.0
($F\bar{4}3m$)	SCAN	6.73	6.73	6.73	60.0	60.0	60.0	0.00	0.1
	r^{2}SCAN	6.71	6.71	6.71	60.0	60.0	60.0	0.00	0.1
CuF_2	Expt.	3.30	4.56	4.64	90.0	83.3	90.0	_	0.73 [11]
(*P21/c*)	SCAN	3.33	4.50	4.54	90.0	83.0	90.0	1.25	0.8
	r^{2}SCAN	3.29	4.53	4.59	90.0	83.1	90.0	0.96	0.8

Density of states calculations

The electronic density of states (DOS) for all TMFs calculated with SCAN, SCAN+U, r^{2}SCAN, r^{2}SCAN+U (for U optimized at 298 K formation enthalpy) are illustrated from Figures S5−S12. For V and Fe-fluorides the calculated DOS with U optimized using experimental data at 0 K and 298 K are depicted in Figures S13 and S14.

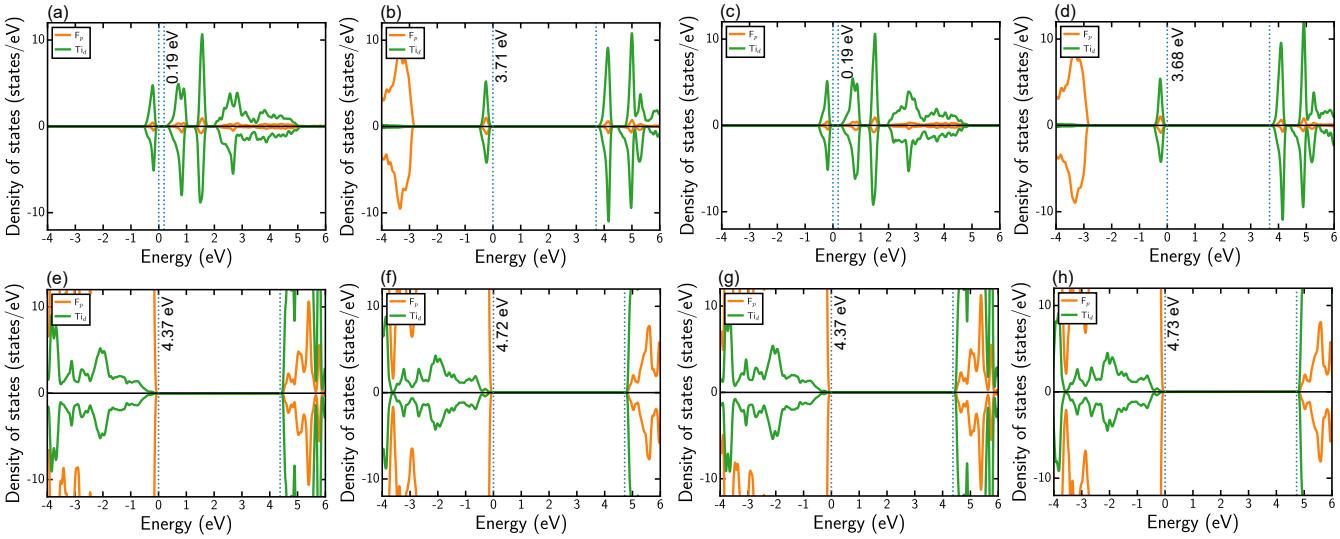

Figure S5: DOS for TiF_3 calculated using (a) SCAN, (b) SCAN+U, (c) r^{2}SCAN and (d) r^{2}SCAN+U. DOS for TiF_4 calculated using (e) SCAN, (f) SCAN+U, (g) r^{2}SCAN and (h) r^{2}SCAN+U. Solid orange and green lines represent F p and transition metal (Ti) d states. Dotted blue lines are band edges, with text notations indicating band gaps. In metallic structures, dashed black lines indicate the Fermi level. The zero of the energy scale is referened to the valence band edge in non-metals and to the Fermi level in metals.

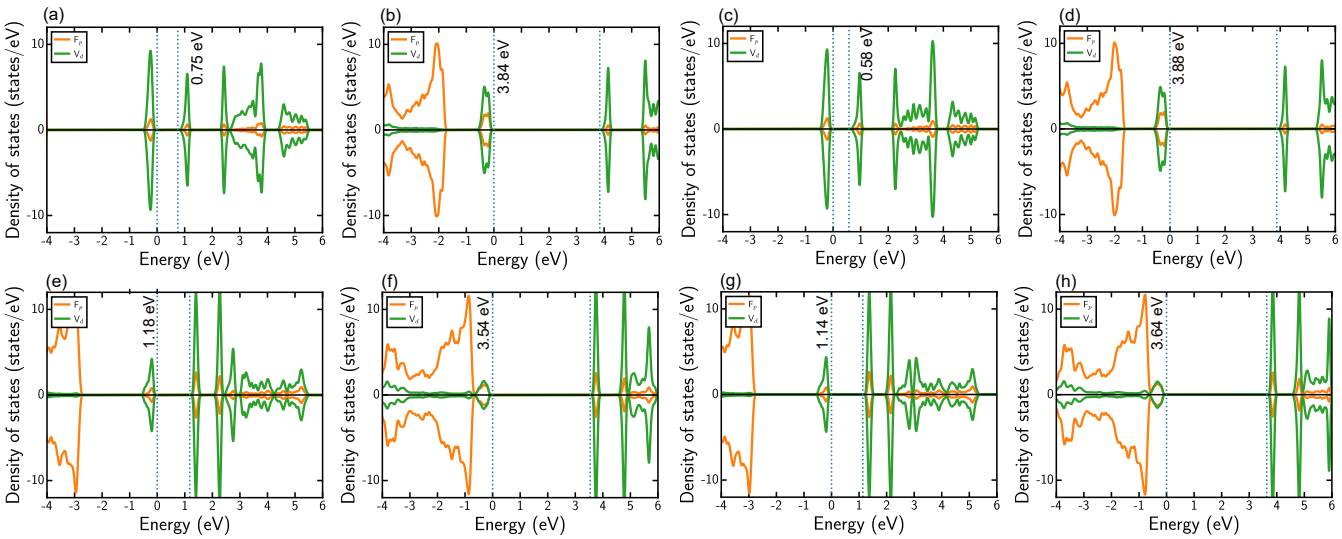

Figure S6: DOS for VF_3 calculated using (a) SCAN, (b) SCAN+U, (c) r^{2}SCAN and (d) r^{2}SCAN+U. DOS for VF_4 calculated using (e) SCAN, (f) SCAN+U, (g) r^{2}SCAN and (h) r^{2}SCAN+U. Notations in each panel are similar to **Figure S5**.

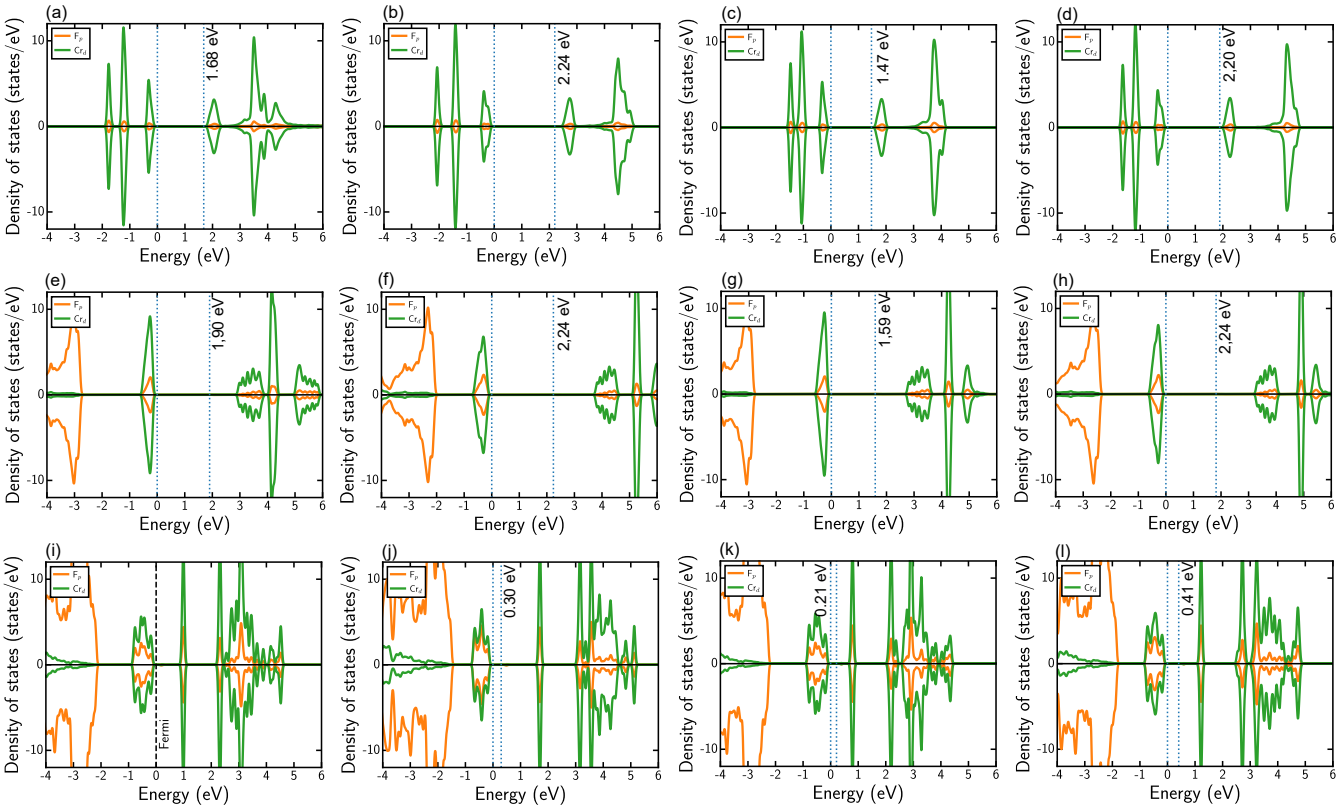

Figure S7: DOS for CrF_2 (top row), CrF_3 (middle row), and CrF_4 (bottom row) calculated using SCAN (panels a, e, and i), SCAN+U (b, f, j), r^{2}SCAN (c, g, k) and r^{2}SCAN+U (d, h, l). Notations in each panel are similar to **Figure S5**.

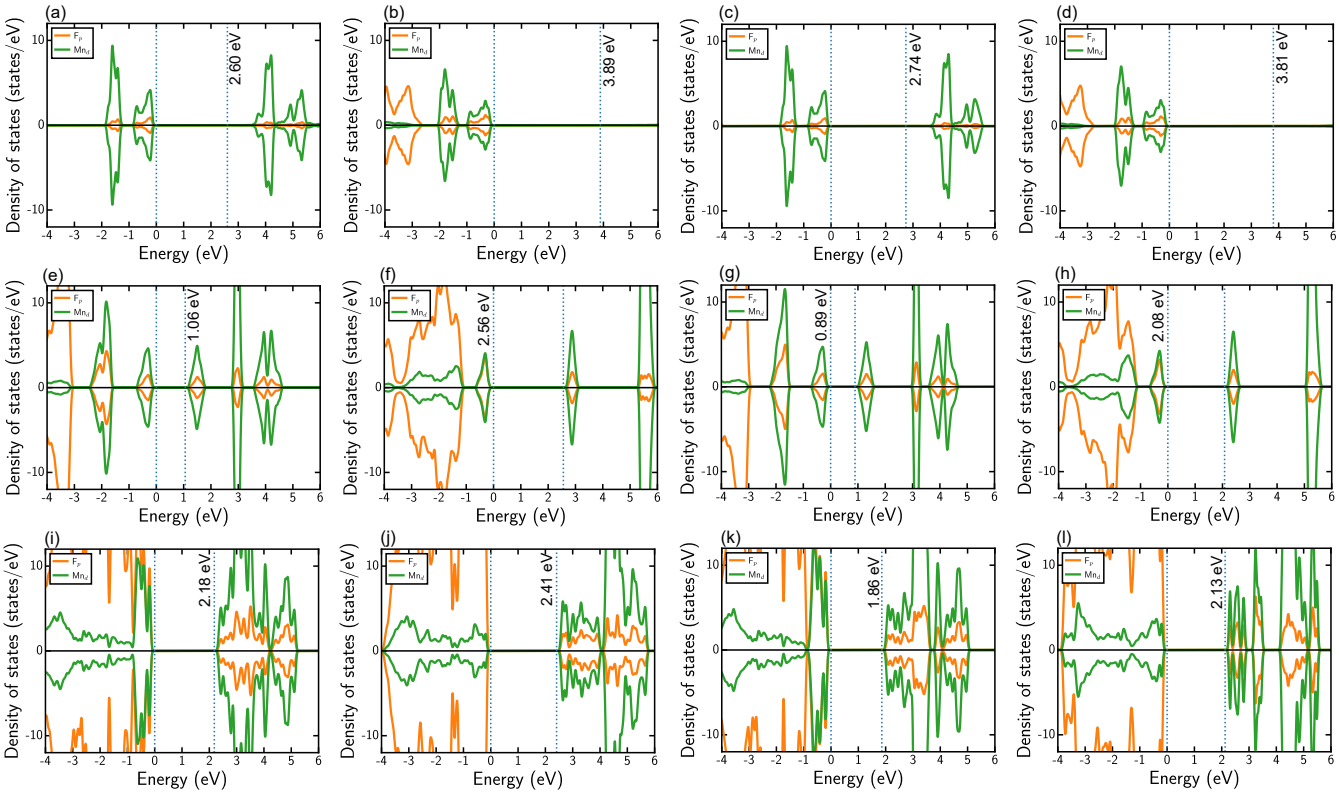

Figure S8: DOS for MnF_2 (top row), MnF_3 (middle row), and MnF_4 (bottom row) calculated using SCAN (panels a, e, and i), SCAN+U (b, f, j), r^{2}SCAN (c, g, k) and r^{2}SCAN+U (d, h, l). Notations in each panel are similar to **Figure S5**.

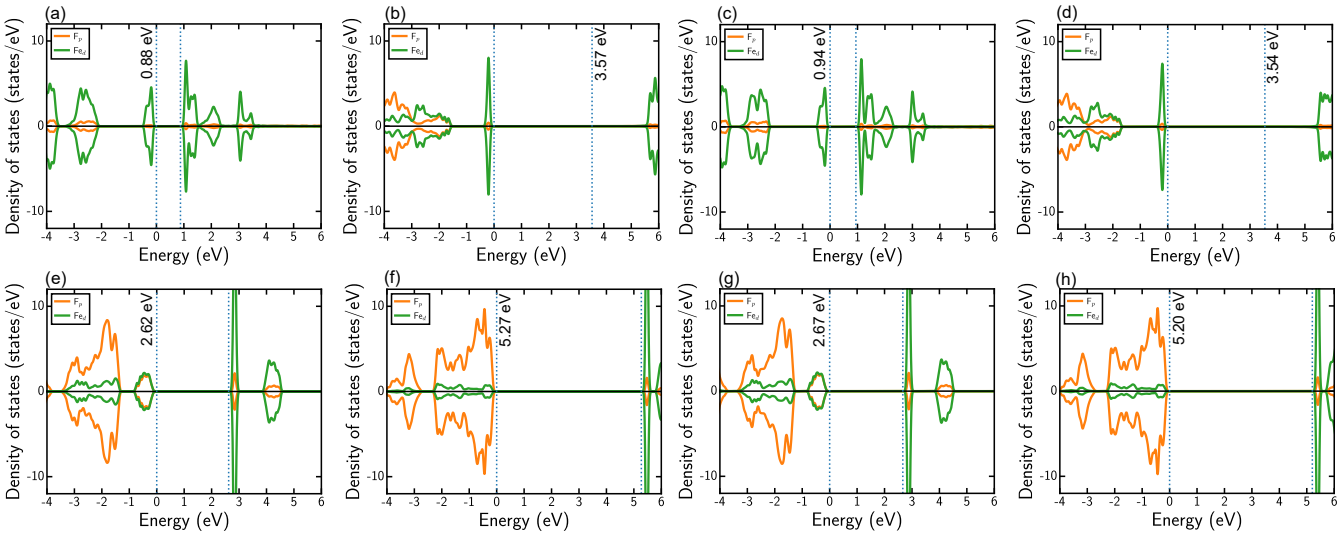

Figure S9: DOS for FeF_2 calculated using (a) SCAN, (b) SCAN+U, (c) r^{2}SCAN and (d) r^{2}SCAN+U. DOS for FeF_3 calculated using (e) SCAN, (f) SCAN+U, (g) r^{2}SCAN and (h) r^{2}SCAN+U. Notations in each panel are similar to **Figure S5**.

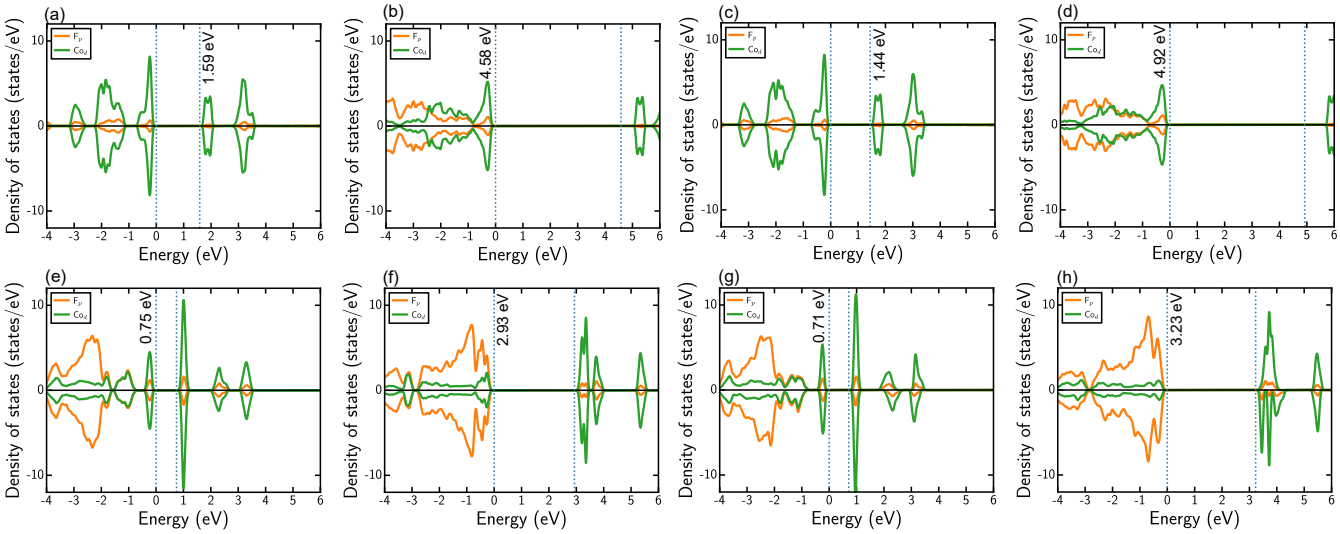

Figure S10: DOS for CoF_2 calculated using (a) SCAN, (b) SCAN+U, (c) r^{2}SCAN and (d) r^{2}SCAN+U. DOS for CoF_3 calculated using (e) SCAN, (f) SCAN+U, (g) r^{2}SCAN and (h) r^{2}SCAN+U. Notations in each panel are similar to **Figure S5**.

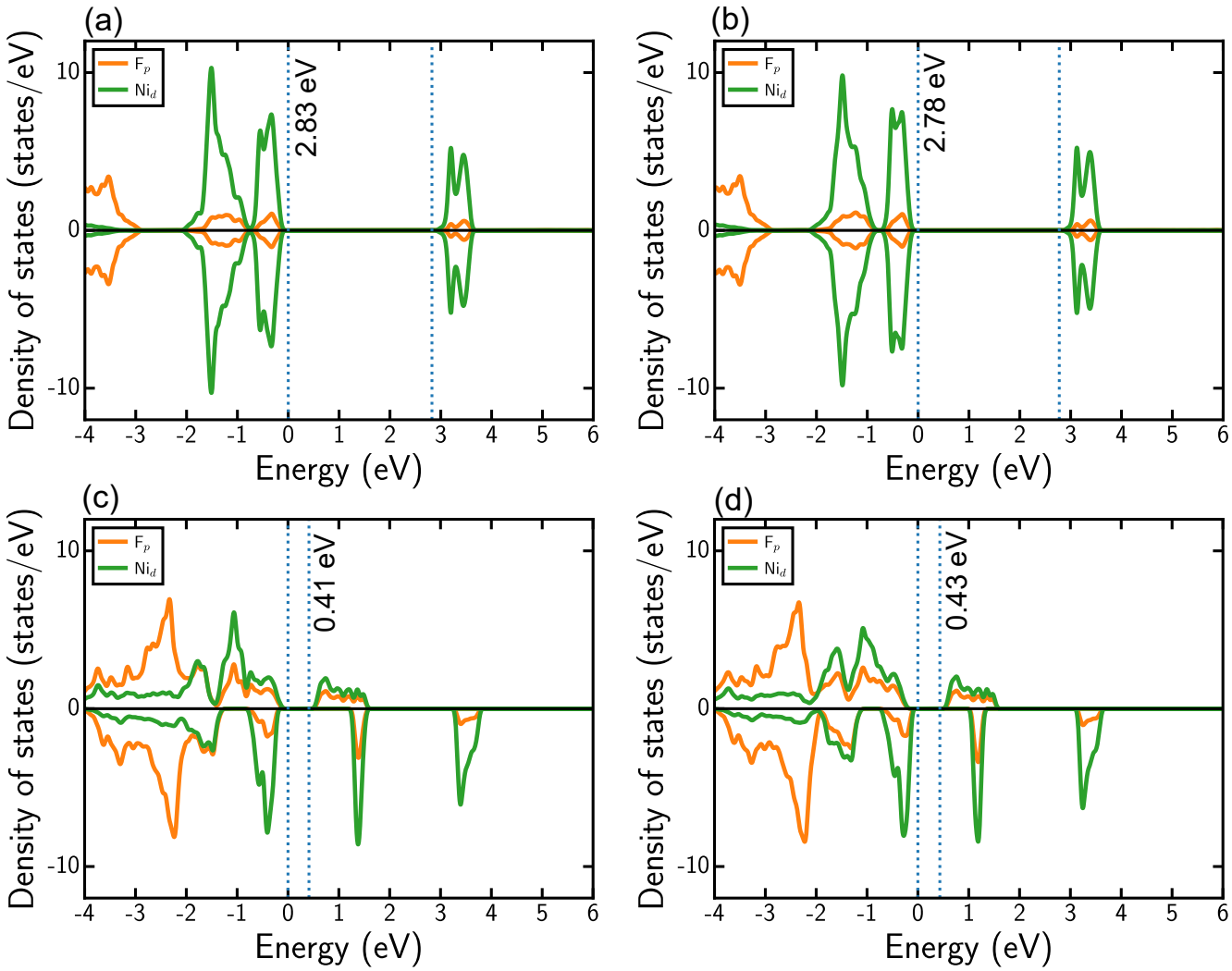

Figure S11: DOS for NiF_2 (panels a, b) and NiF_3 (c, d) calculated using SCAN (panels a, c), and r^2SCAN (b, d). Notations in each panel are similar to **Figure S5**.

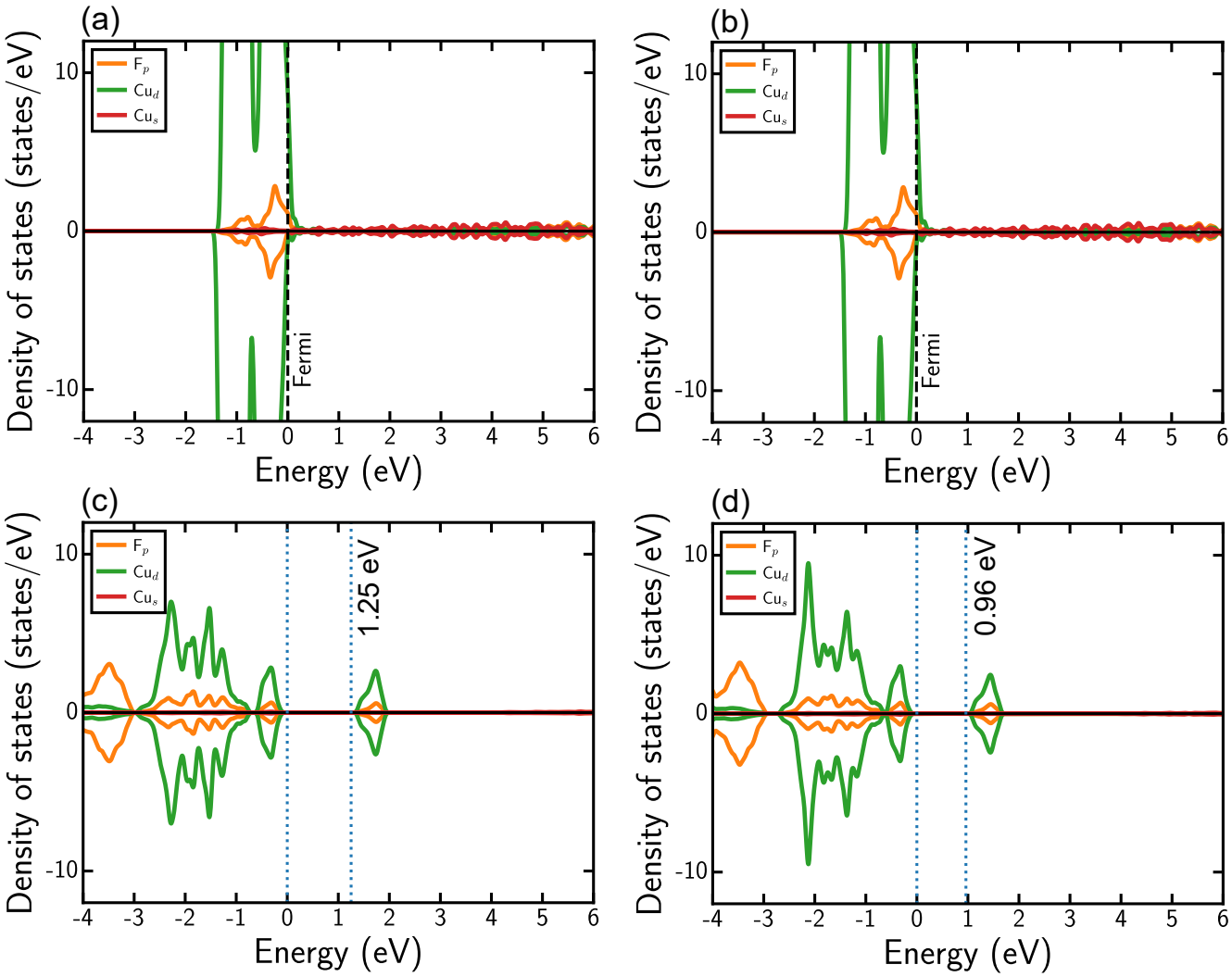

Figure S12: DOS for CuF (panels a, b) and CuF_2 (c, d) calculated using SCAN (panels a, c), and r^{2}SCAN (b, d). Notations in each panel are similar to **Figure S5** Solid red lines represent Cu 4*s* states.

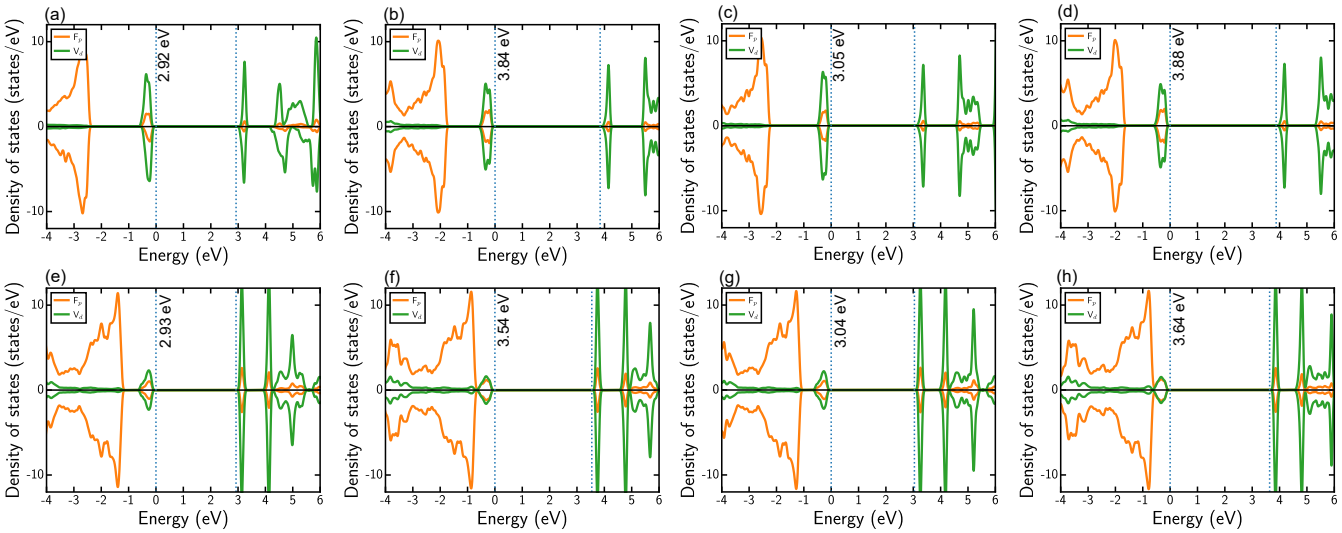

Figure S13: Comparison of DOS for VF_3 (top row) and VF_4 (bottom row) calculated using SCAN+U with U optimized using experimental data at (panels a, e) 0 K and (b , f) 298 K, and r^{2}SCAN+U with U optimized using experimental data at (c, g) 0 K and (d, h) 298 K. Notations in each panel are similar to **Figure S5**.

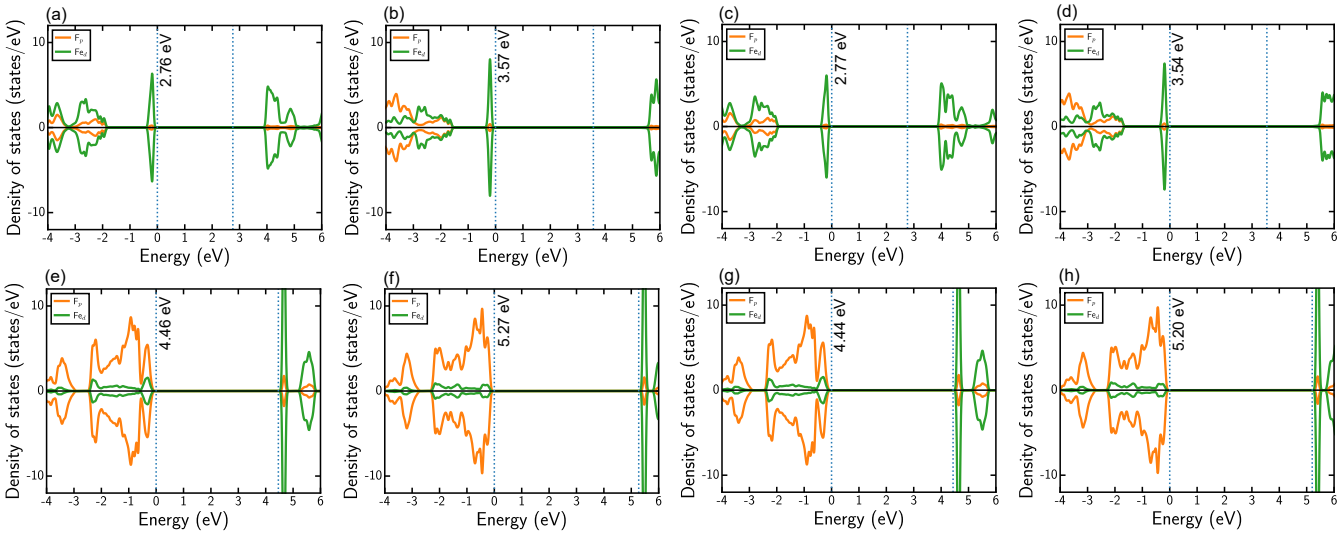

Figure S14: Comparison of DOS for FeF_2 (top row) and FeF_3 (bottom row) calculated using SCAN+U with U optimized using experimental data at (panels a, e) 0 K and (b , f) 298 K, and r^{2}SCAN+U with U optimized using experimental data at (c, g) 0 K and (d, h) 298 K. Notations in each panel are similar to **Figure S5**.

Powder colors and band gaps

The estimated empirical band gap values of most TMFs lies within the range of 1.6 and 3.2 eV. For instance, the colour of TiF_3, MnF_4 and CrF_2 lies in the violet, blue and green-blue colour spectrum which corresponds to a band gap of ∼3.1, ∼2.7 and ∼2.4 eV, respectively, while for VF_4, CrF_3, CrF_4, FeF_3 lies in the blue (corresponds to band gap of ∼2.2 eV) colour spectrum. Similarly, the colour of VF_3 and NiF_2, CoF_3 is lies in the green-yellow (∼2.1 eV), yellow (∼1.9 eV), and brown (∼1.8 eV) colour spectrum, respectively, while MnF_2, MnF_3, CoF_2 is red (∼1.7 eV). Whereas the band gap of NiF_3 is approximated ∼1.0 eV, due to its black powder colour appearance. Note that a material with black powder colour might also corresponds to a metallic character or zero band gap.

Table S4: Powder sample colors of binary TMFs and corresponding numerically approximated band gap values from literature sources.

Compound	Powder sample colors	Estimated band gap (eV)
TiF_3	Violet [12]	3.1
TiF_4	White [12]	3.2
VF_3	Yellow-green [12]	2.1
VF_4	Green [12]	2.3
CrF_2	Green-blue [12]	2.5
CrF_3	Green [12]	2.3
CrF_4	Green [12]	2.3
MnF_2	Red [12]	1.7
MnF_3	Red [12]	1.7
MnF_4	Blue [12, 13]	2.7
FeF_2	White [12]	3.2
FeF_3	Green [12]	2.3
CoF_2	Red [12]	1.6
CoF_3	Brown [12]	1.8
NiF_2	Yellow [12]	2.1
NiF_3	Black [12, 14]	1.6
CuF	White [12]	3.2
CuF_2	White [12]	3.2

U with 298 K data versus U with 0 K data

Table S5: Comparison of calculated and experimental lattice parameters, on-site magnetic moments, and band gaps for V- and Fe-fluorides. Calculated values with optimal U derived using experimental data at 0 K and 298 K are listed for both SCAN+U and r^{2}SCAN+U.

Composition		Source	Lattice constants (Å)			Band gap (eV)	On-site magnetic moment (μ_B)
			a	b	c		
VF_3		Expt.	5.37	5.37	5.37	_	2.0 [2]
	U at 298 K	SCAN+U	5.41	5.41	5.41	3.84	1.9
		r^{2}SCAN+U	5.44	5.44	5.44	3.88	1.9
	U at 0 K	SCAN+U	5.38	5.41	5.38	2.92	1.9
		r^{2}SCAN+U	5.41	5.42	5.41	3.05	1.9
VF_4		Expt.	5.38	5.17	5.34	_	1.0 [3]
	U at 298 K	SCAN+U	5.34	5.20	5.30	3.54	1.0
		r^{2}SCAN+U	5.36	5.21	5.32	3.64	1.0
	U at 0 K	SCAN+U	5.31	5.19	5.27	2.93	1.0
		r^{2}SCAN+U	5.34	5.20	5.33	3.04	1.0
FeF_2		Expt.	4.70	4.70	3.31	_	3.8 [7]
	U at 298 K	SCAN+U	4.70	4.70	3.30	3.57	3.8
		r^{2}SCAN+U	4.72	4.72	3.30	3.54	3.8
	U at 0 K	SCAN+U	4.68	4.69	3.30	2.76	3.8
		r^{2}SCAN+U	4.70	4.70	3.31	2.77	3.8
FeF_3		Expt.	5.36	5.36	5.36	_	5.0 [2]
	U at 298 K	SCAN+U	5.36	5.36	5.36	5.27	4.5
		r^{2}SCAN+U	5.37	5.37	5.37	5.20	4.5
	U at 0 K	SCAN+U	5.36	5.36	5.36	4.46	4.4
		r^{2}SCAN+U	5.37	5.37	5.37	4.44	4.4

Band gap comparisons

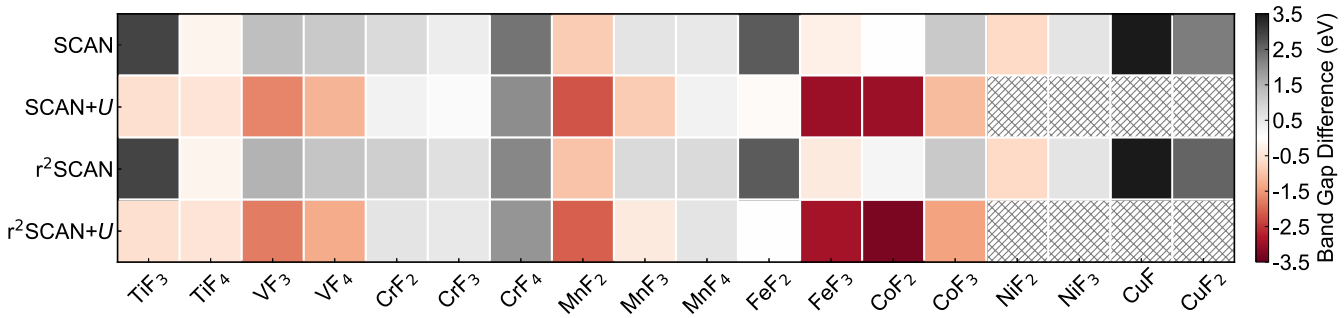

Figure S15: Band gap difference (in eV) across all TMFs considered between the experimental (approximated from powder sample color) and computed values using SCAN (first row), SCAN+U(second), r^{2}SCAN (third), and r^{2}SCAN+U (fourth) are displayed. We define the difference as the experimental gap minus the calculated gap. The grey (red) square boxes indicates an underestimation (overestimation) of the calculated gaps against the experimental gaps. Hatched squares in second and fourth rows indicate absence of SCAN+U and r^{2}SCAN+U calculations, since a U correction is not required for Ni and Cu fluorides.

Table S6: Comparison of SCAN, SCAN+U, r^{2}SCAN and r^{2}SCAN+U calculated band gaps with hybrid functional (HSE06) for TiF_3, FeF_2 and CoF_2. Additionally, we compared our calculated band gaps in VF_3, CrF_3, MnF_3, FeF_3, CoF_3, and NiF_3 against computed HSE06 band gaps reported in Ref [15]

. We used the U values optimized using experimental data at 298 K for the comparison here.

Systems	Calculated band gaps (eV)				
	HSE06	SCAN	SCAN+U	r^{2}SCAN	r^{2}SCAN+U
TiF3	2.54, 2.87 [15]	0.19	3.71	0.19	3.68
FeF2	3.23	0.88	3.57	0.94	3.54
CoF2	4.48	1.59	4.58	1.44	4.92
VF3	3.40 [15]	0.8	3.8	0.6	3.9
CrF3	4.91 [15]	1.9	2.2	1.6	1.8
MnF3	3.03 [15]	1.1	2.6	0.9	2.1
FeF3	5.35 [15]	2.6	5.3	2.7	5.2
CoF3	3.95 [15]	0.7	2.9	0.7	3.2
NiF3	3.28 [15]	0.4	-	0.4	-

Average voltage calculations

The reaction involving an insertion/extraction of Na^+ in an iron fluoride cathode during discharging/charging process can be represented by the redox reaction in Equation 1:

$$FeF_3 + Na^+ + e^- \rightleftharpoons NaFeF_3 \tag{1}$$

The average intercalation voltage due to (de)intercalation of one mole of Na^+ can be calculated using the Nernst equation (Equation 2) as follows:

$$\langle V \rangle = -\frac{\Delta G}{F} \approx -\frac{E(NaFeF_3) - [E(FeF_3) + \mu_{Na}]}{F} \tag{2}$$

Where ΔG is the Gibbs energy change, which is approximated by the total energy (E) change as calculated by DFT (i.e., $\Delta G \approx \Delta E$), F is the Faraday constant, and μ_{Na} is the Na chemical potential in pure Na metal.

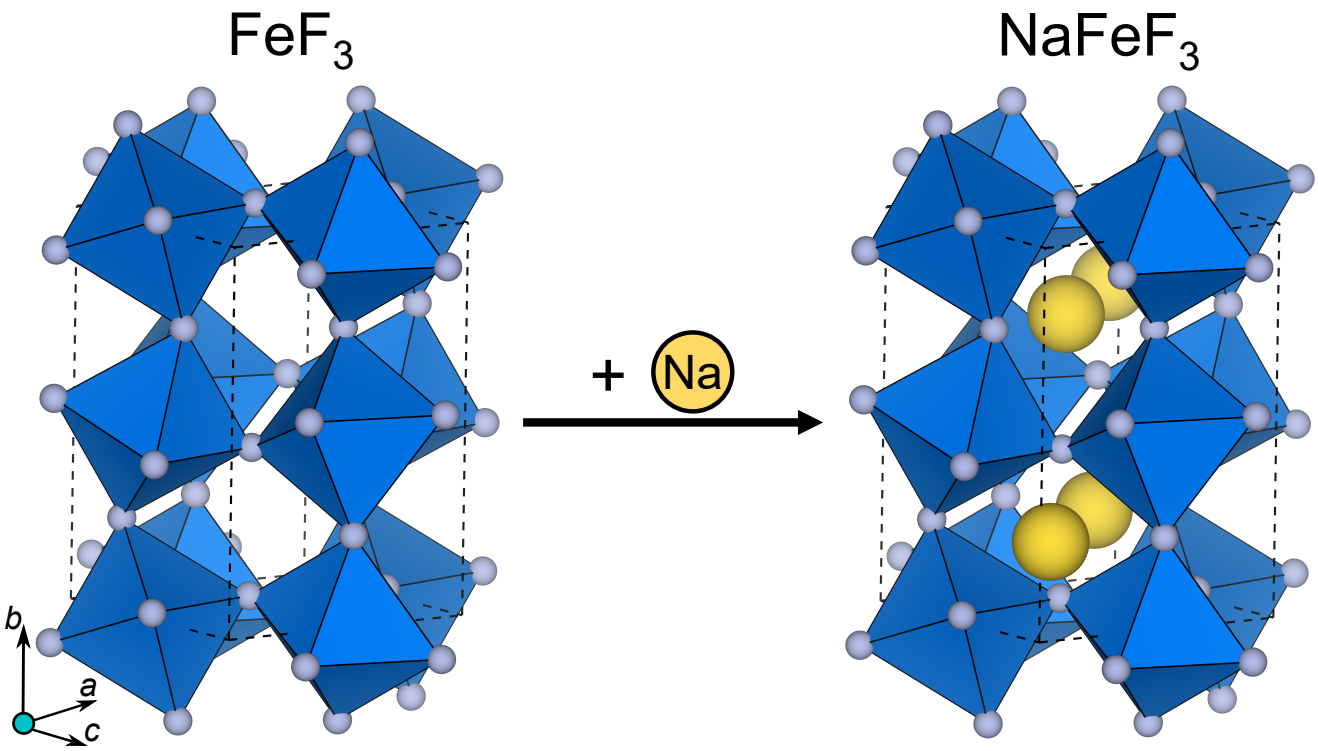

Figure S16: Structure of fully charged (FeF_3) and discharged ($NaFeF_3$) phase of iron fluoride cathode, for a topotactic Na intercalation. Na and F are indicated by yellow and grey spheres, respectively, while the FeF_6 octahedra are represented by blue polyhedra. $NaFeF_3$ adopts an orthorhombically-distorted perovskite structure (space group: *Pnma*).

Linear response theory calculations

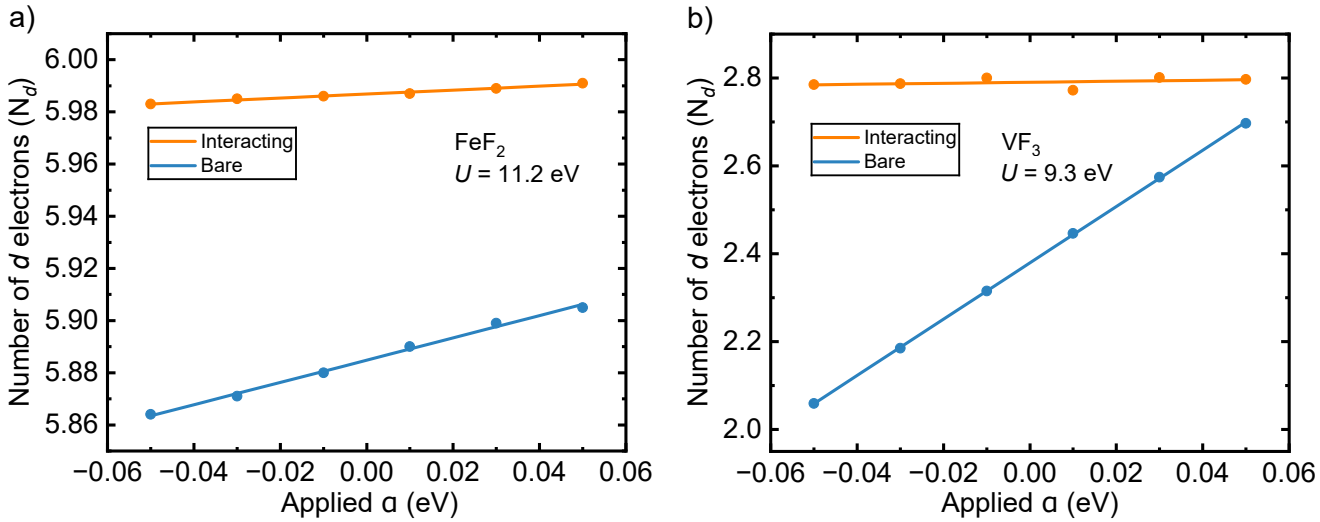

Figure S17: Determination of Hubbard U for FeF_2 and VF_3 using the linear response method and the SCAN functional within a smaller range of α values.

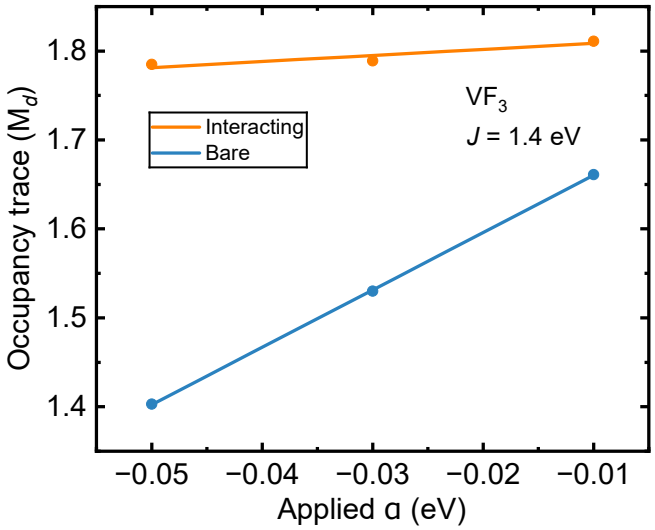

Figure S18: Determination of Hund's J for VF_3 using the linear response method and the SCAN functional. The panel depicts the variation in the on-site magnetic moment (M_d) within the d orbitals of a single TM site, as a function of the applied perturbation (α in eV).

Hybrid functional calculations

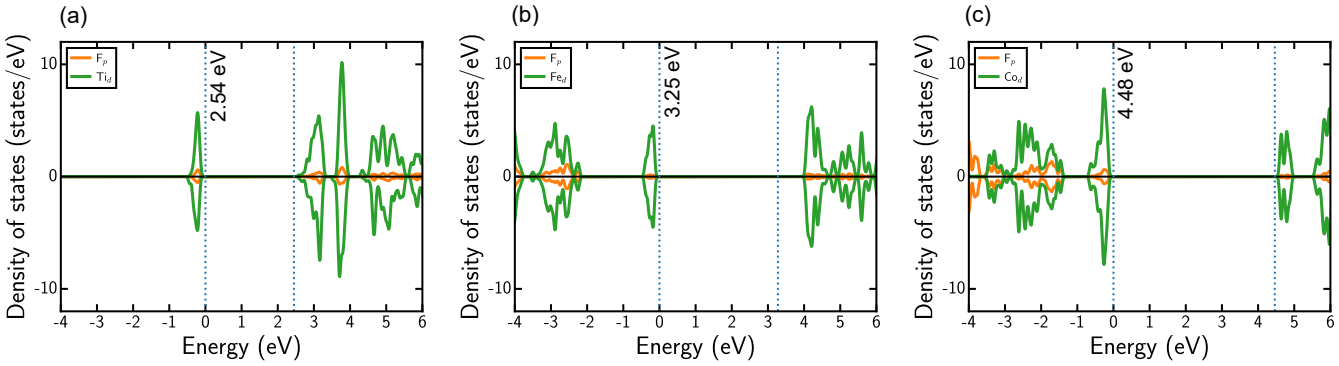

Figure S19: Calculated DOS for (a) TiF_3, (b) FeF_2, and (c) CoF_2 calculated using the HSE06 functional. Notations in each panel are similar to **Figure S5**.

Charge density difference

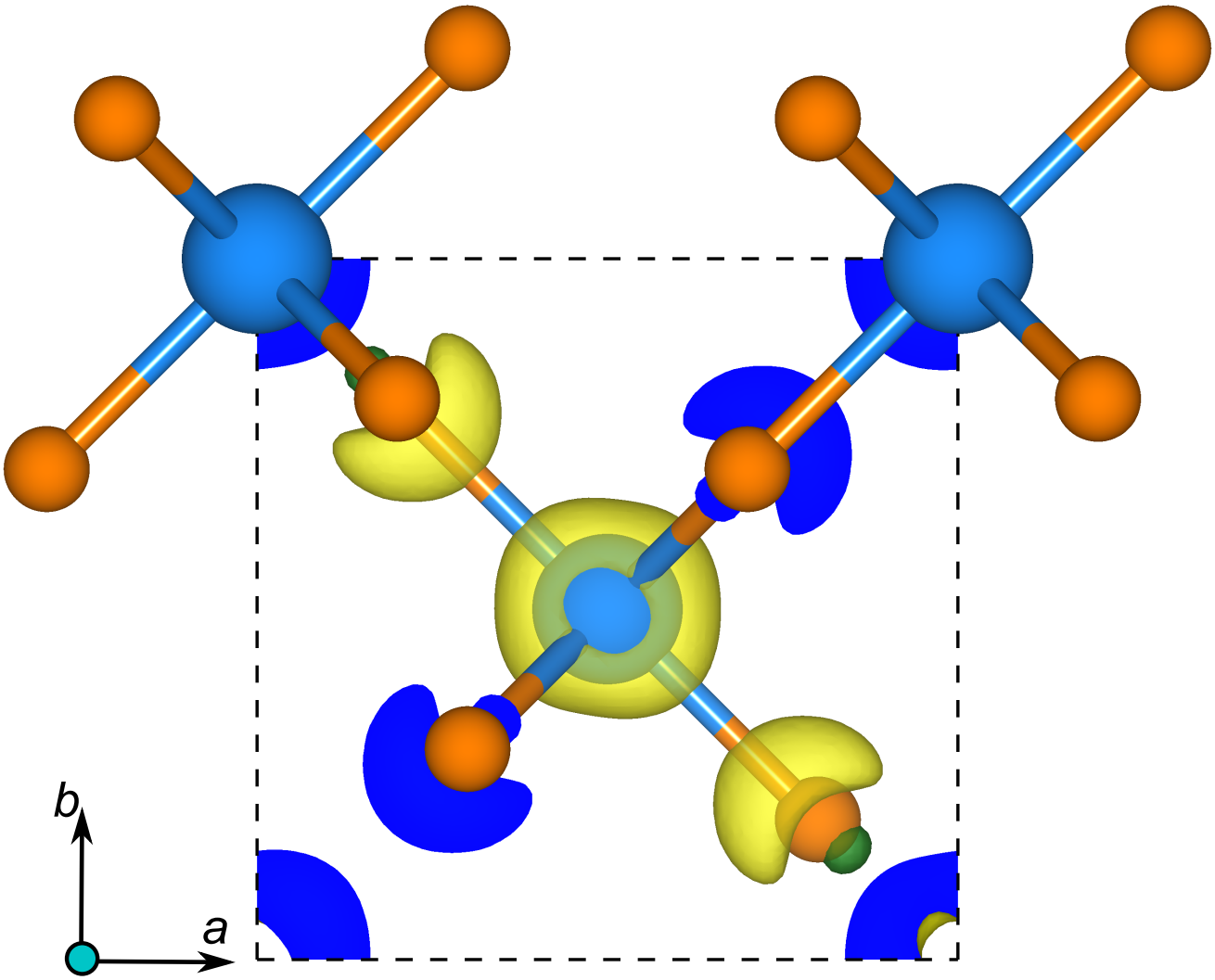

Figure S20: Differential charge density isosurface plotted for FeF_2 by subtracting the charge density of SCAN+U from SCAN. The yellow (green) isosurface corresponds to a negative (positive) net charge difference (of 0.01 e^- $Bohr^{-3}$), while the cross section of the isosurface is illustrated in blue. The Fe and F atoms are represented by light blue and orange spheres, respectively.

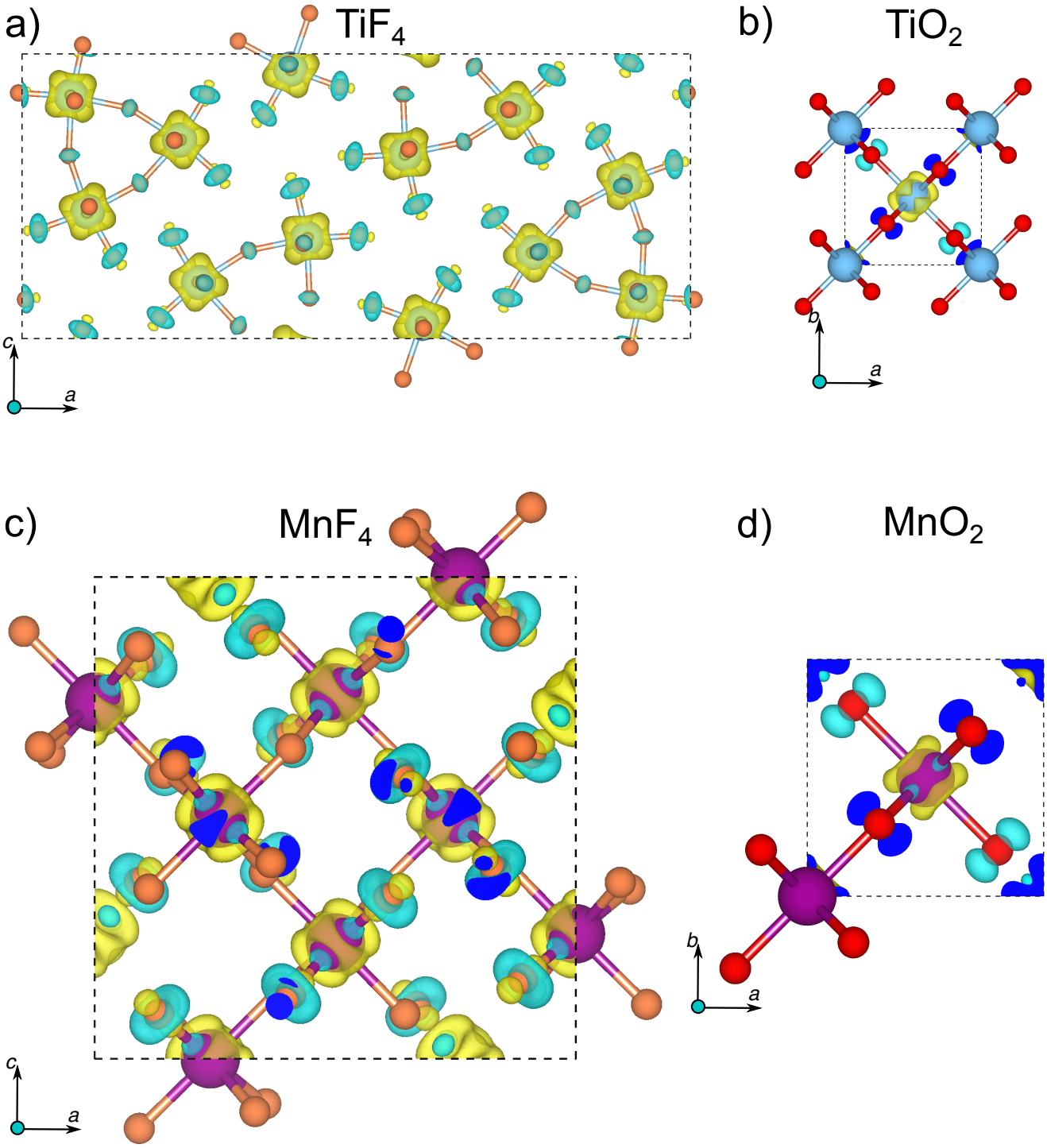

Figure S21: Differential charge density isosurface plotted for (a) TiF_4, (b) TiO_2, (c) MnF_4, and (d) MnO_2 by subtracting the charge density of SCAN+U from SCAN. The yellow (cyan) isosurface corresponds to a negative (positive) net charge difference (of 0.002 e^- $Bohr^{-3}$), while the cross section of the isosurface is illustrated in blue. The light blue, maroon, orange and red spheres represent Ti, Mn, F, and O atoms, respectively.

Convex hull calculations

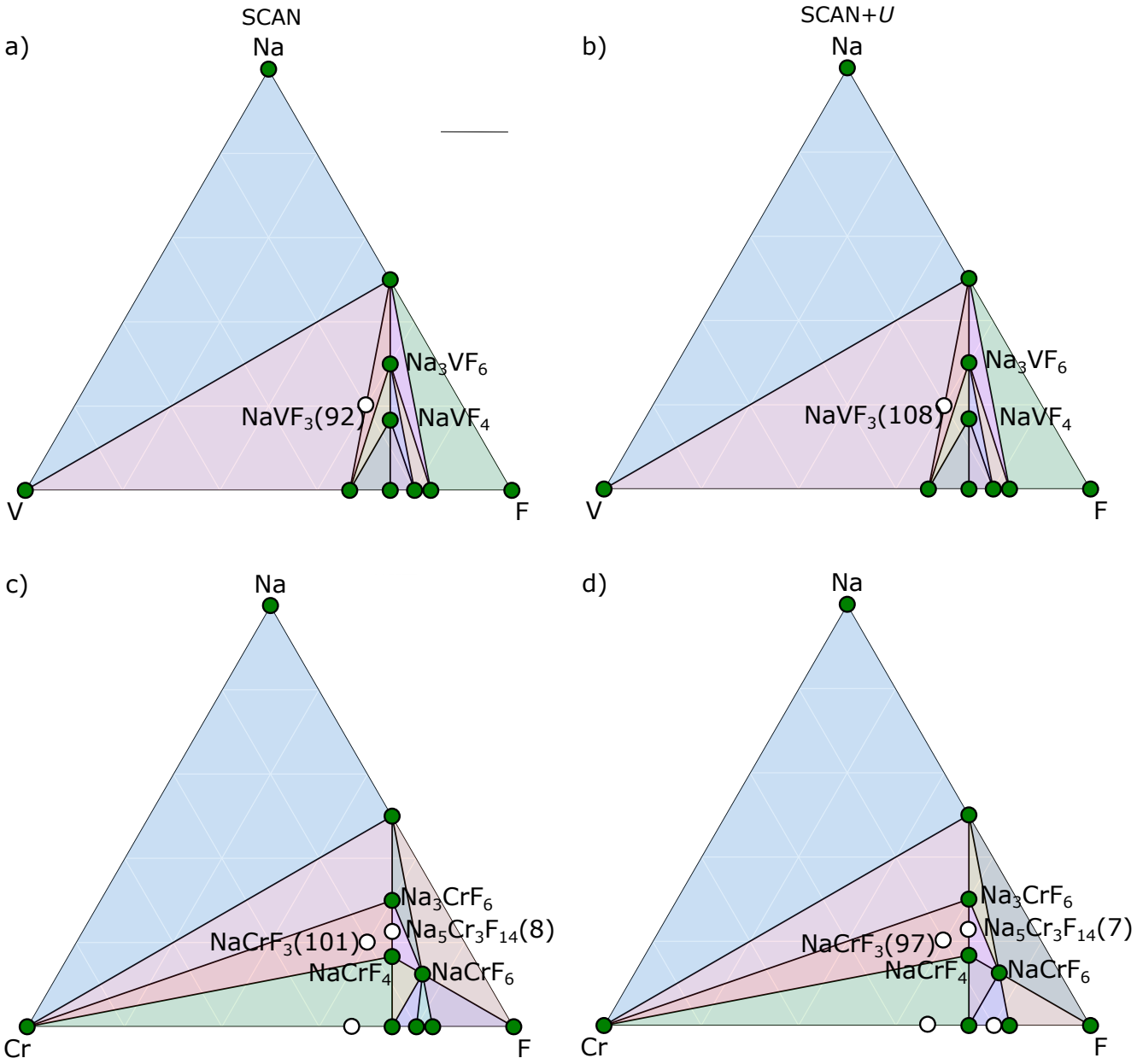

Figure S22: 0 K ternary Na-M-F phase diagrams calculated using SCAN (panels a and c) and SCAN+U (b and d), where M = V (a and b), and Cr (c and d). Stable entities within each phase diagram are indicated by green circles. Black lines connecting different compositions are tie-lines. Unstable/metastable phases are indicated by hollow circles, with the energy above the convex hull (E^{hull}) provided in parenthesis.

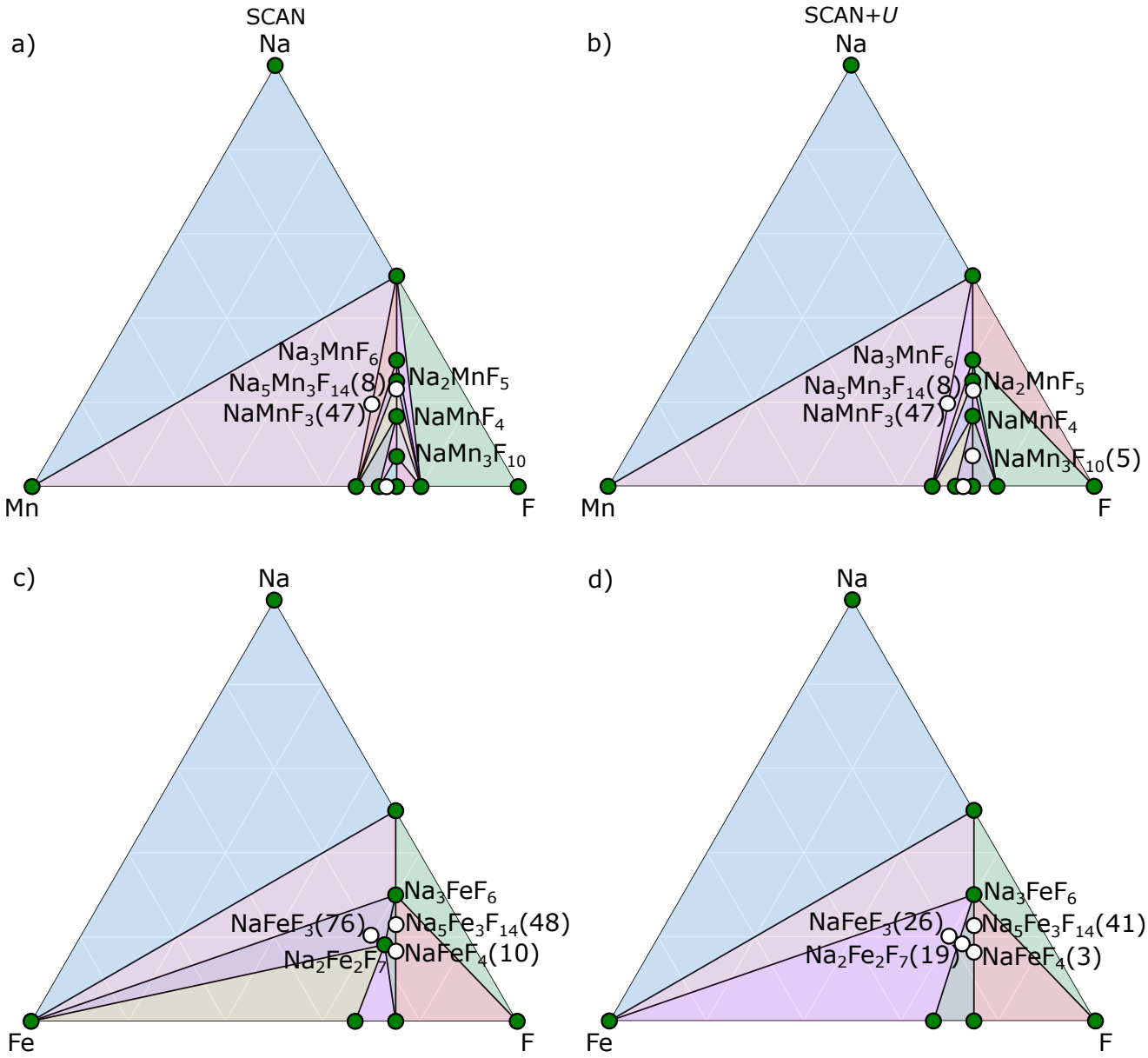

Figure S23: SCAN (panels and c) and SCAN+U (b and d) calculated 0 K ternary Na-M-F phase diagrams, where M = Mn (a and b), and Fe (c and d). Notations in the figure are identical to **Figure S22**.

References

[1] Muratahan Aykol and C Wolverton. Local environment dependent gga+ u method for accurate thermochemistry of transition metal compounds. *Physical Review B*, 90(11):115105, 2014.

[2] EO Wollan, HR Child, WC Koehler, and MK Wilkinson. Antiferromagnetic properties of the iron group trifluorides. *Physical Review*, 112(4):1132, 1958.

[3] AC Gossard, FJ Di Salvo, WE Falconer, TM Rice, JM Voorhoeve, and H Yasuoka. Magnetic ordering of a d1 compound: Vf4. *Solid State Communications*, 14(11):1207–1211, 1974.

[4] Tapan Chatterji and Thomas C Hansen. Magnetoelastic effects in jahn–teller distorted crf2 and cuf2 studied by neutron powder diffraction. *Journal of Physics: Condensed Matter*, 23(27):276007, 2011.

[5] J Strempfer, U Rütt, SP Bayrakci, Th Brückel, and W Jauch. Magnetic properties of transition metal fluorides m f 2 (m= mn, fe, co, ni) via high-energy photon diffraction. *Physical Review B*, 69(1):014417, 2004.

[6] Karel Lutar, Adolf Jesih, and Boris Žemva. Krf2/mnf4 adducts from krf2/mnf2 interaction in hf as a route to high purity mnf4. *Polyhedron*, 7(13):1217–1219, 1988.

[7] Zhen-hua YANG, Xian-you WANG, Liu Li, and Xu-ping SU. Structural, magnetic and electronic properties of fef2 by first-principle calculation. *Transactions of Nonferrous Metals Society of China*, 22(2):386–390, 2012.

[8] Tapan Chatterji, Bachir Ouladdiaf, and Thomas C Hansen. The magnetoelastic effect in cof2 investigated by means of neutron powder diffraction. *Journal of Physics: Condensed Matter*, 22(9):096001, 2010.

[9] Sanghyun Lee, Shuki Torii, Yoshihisa Ishikawa, Masao Yonemura, Taketo Moyoshi, and Takashi Kamiyama. Weak-ferromagnetism of cof3 and fef3. *Physica B: Condensed Matter*, 551:94–97, 2018.

[10] Tapan Chatterji, Gail N Iles, Bachir Ouladdiaf, and Thomas C Hansen. Magnetoelastic effect in mf2 (m= mn, fe, ni) investigated by neutron powder diffraction. *Journal of Physics: Condensed Matter*, 22(31):316001, 2010.

[11] P Fischer, W Hälg, D Schwarzenbach, and H Gamsjäger. Magnetic and crystal structure of copper (ii) fluoride. *Journal of Physics and Chemistry of Solids*, 35(12):1683–1689, 1974.

[12] David R Lide. *CRC handbook of chemistry and physics*, volume 85. CRC press, 2004.

[13] Florian Kraus, Sergei I Ivlev, Jascha Bandemehr, Malte Sachs, Clemens Pietzonka, Matthias Conrad, Michael Serafin, and Bernd G Müller. Synthesis and characterization of manganese tetrafluoride β-mnf4. *Zeitschrift für anorganische und allgemeine Chemie*, 646(18):1481–1489, 2020.

[14] MI Nikitin and AS Alikhanyan. Thermochemistry of nickel trifluoride. *Russian Journal of Inorganic Chemistry*, 64:641–644, 2019.

[15] Stefan Mattsson and Beate Paulus. Density functional theory calculations of structural, electronic, and magnetic properties of the 3d metal trifluorides mf3 (m= ti-ni) in the solid state. *Journal of computational chemistry*, 40(11):1190–1197, 2019.